Standoff UV-C imaging of alpha particle emitters

Krasniqi, Faton S.

2021-01-21

Standoff UV-C imaging of alpha particle emitters

Faton S. Krasniqi [a,*], Thomas Kerst [b,c], Martti Leino [b], Jens-Tarek Eisheh [d], Harri Toivonen [e], Annette Röttger [a], Juha Toivonen [b,*]

[a] *Physikalisch-Technische Bundesanstalt (PTB), Bundesallee 100, 38116 Braunschweig, Germany*
[b] *Photonics Laboratory, Physics Unit, Tampere University, 33101 Tampere, Finland*
[c] *Helsinki Institute of Physics, Gustaf Hällströmin katu 2, 00014 Helsinki, Finland*
[d] *Bundesamt für Strahlenschutz, Willy-Brandt-Straße 5, 38226 Salzgitter, Germany*
[e] *HT Nuclear Ltd, Notkokatu 4, 05880 Hyvinkää, Finland*

ARTICLE INFO

ABSTRACT

Alpha particles are proven to be very useful in many areas of medicine, technology and science. Yet, they represent the biggest risk to soft biological tissues compared to all nuclear decay products when ingested or inhaled, implying thus stringent radiation protection measures in the management and monitoring of samples that emit them. In this paper we present a standoff optical imaging approach that enables sensing of a radiological threat items at facilities where alpha-emitting material is manufactured, handled, used and stored, at safe distances without putting personnel at risk or contaminating equipment. The optical imaging of alpha-emitting samples is based on the radiation induced air luminescence (radioluminescence) in the UV-C (solar-blind) spectral region which enables detection of alpha particles even under bright light conditions. We show that by adding trace amounts of nitric oxide into the nitrogen atmosphere surrounding the sample, alpha sources with specific activities as low as 1.5 Bq/cm^2 can be remotely imaged. This work provides a proof-of-concept implementation of a novel imaging approach that not only enhances capabilities of a state to take actions which effectively mitigate consequences of an radiological emergency for the society, health, environment and economy, but also benefits nuclear industry in decommissioning efforts.

1. Introduction

Fabrication, handling, and storage of alpha-emitting materials carries considerable potential for radiological accidents [1–3]. Therefore, to reduce the potential risk of human exposure and possible contamination of the environment, a standoff detection system which identifies possible threats from a distance, without a human involvement, is essential. This demand is mainly driven by the fact that alpha particles represent the biggest risk to biological tissue compared to all nuclear decay products due to their high energy, large mass and charge density. The average energy deposited along their track (the linear energy transfer) scales as Q^2/v^2, with Q being the charge of the alpha particle and v its velocity, is very high, making them thus highly ionizing [4]. Owing to the very high concentration of energy deposited along their track, alpha particles have a high probability of promoting double stranded deoxyribonucleic acid (DNA) breaks, an almost irreparable damage, making them very cytotoxic [5]. In a biological soft tissue, for example, the complete energy of an alpha particle is dissipated within a very short path length, which is often less than 100 μm (i.e. only few cell diameters), implying thus that a single alpha particle has the ability to kill all cells within its range (typically, two to four cells) [3].

Standoff systems detect alpha particles indirectly by utilizing physical effects such as alpha-particle-induced luminescence (radioluminescence), laser probing of alpha-induced excited state of air molecules, and laser probing of collisional ionization (breakdown) of the air [6–17]. While laser based methods [16–19] are still at their infancy, the radioluminescence technique is already in a mature stage with its feasibility demonstrated in many experiments [6–15,20,21]. Radioluminescence in air is generated mostly by emission of molecular nitrogen (N_2), and to much lesser extend, by trace amounts of nitric oxide (NO) in air, with wavelength spanning three ultraviolet (UV) bands and about 99% of emission occurring in the 280–440 nm spectral range [6–8].

The challenges for a remote optical detection of alpha emitting radionuclides are significant, primarily because the spectrum of radioluminescent light falls within the range of solar radiation wavelengths and is eclipsed by it due to much greater solar irradiance at wavelengths longer than 280 nm [6,7,11]. In the UV-C spectral region, on the other hand, the background light is very low, in particular in daylight, because most of solar radiation below 280 nm is absorbed

by the atmospheric ozone [6,7,11,12]; The intensity of UV-C radio-luminescence, however, is very low (<1%). Thus, both cases impose strict limitation to the wide application of this technique. A major breakthrough that opened the opportunity for overcoming the above fundamental limitations was reported by Kerst et al. [11] who showed that by adding trace amounts of nitric oxide into nitrogen atmosphere surrounding the sample, the overall radioluminescence yield increases about 25-fold, with almost all of the emission located in the UV-C spectral region.

In this work we present the radioluminescence imaging of alpha emitting sources in the UV-C spectral region, between 250 and 280 nm. An optical detection system consisting of an intensified charge-coupled device (CCD) camera, an interference UV-C filter and imaging optics has been used to image the radioluminescence of gas molecules surrounding Am-241 sources. We experimentally demonstrate that a nitrogen purge with as low as 3 ppm nitric oxide impurities enables imaging of low activity samples, for example, those used in smoke detector ionizers. By using larger receiving optics and an optical system based on an optimized Galilean-like telescope [7,10], the detection limit of about 330 Bq was reached. Here, the UV-C radioluminescence from a wide area reference source of natural uranium with specific activity of about 1.5 Bq/cm^2 was still visible.

The alpha imaging concept has been demonstrated in a number of experiments using both conventional film photography techniques and CCD camera technology [6,7,9,15,20,21]. However, since the presence of UV photons from the background light (e.g. sunlight or man-made sources) superseeds the faint radioluminescence signal, this imaging approach was limited only to very dark environment where almost complete darkness is ensured. In another attempt, Ivanov et al. [21] used UV-C CCD camera to image alpha-induced air-fluorescence in daylight conditions, yet, due to the fact that only a small portion of air radioluminescence is located in the UV-C region, the ability to detect weaker alpha sources is severely limited. Radioluminescence images originating from a liquid sample composed of Am-241 dissolved in an aqueous nitric acid (HNO$_3$) solution were also reported [22]. They show an uniform distribution of radioluminescence throughout the sample volume with a slight increase at the surface of the liquid interfacing with air.

2. Experimental setup

The scheme of the experimental setup is shown in Fig. 1a. Alpha emitting samples were imaged using two optical detection systems: (*i*) a wide field-of-view (FOV) imaging system in conjunction with an intensified CCD camera (hereafter, CCD-based imaging system) and (*ii*) a narrow FOV Galilean-type telescope combined with a cesium-telluride photocathode photomultiplier (hereafter, scanning PMT system). While in the first case the ICCD camera captures the image of the whole scene contained within the angle of view, the PMT based system in (*ii*) produces radioluminescence images by scanning its narrow FOV over the user-defined region of interest while recording the photon count rate point-by-point [10].

2.1. CCD-based imaging system

The imaging optics employed in the CCD-based setup has a diameter of 2 inches and it consists of two lenses (Thorlabs LA4545-UV, f=100 mm and LA4052-UV, f = 35 mm) which guide the radioluminescence light to the imaging sensor. A 2-inch UV-C filter (Materon F-SP-0005934) with a pass-band close to 270 nm (see Fig. 1b) is mounted in front of the camera lens system. The images of alpha sources were captured by the intensified CCD (ICCD) camera iStar 340T from Andor Corporation. In this camera type, an image intensifier which comprises a photocathode, microchannel plate (MCP) and a phosphor screen, optically coupled to the CCD chip is utilized to increase the sensitivity down to single photon level. The gain of the
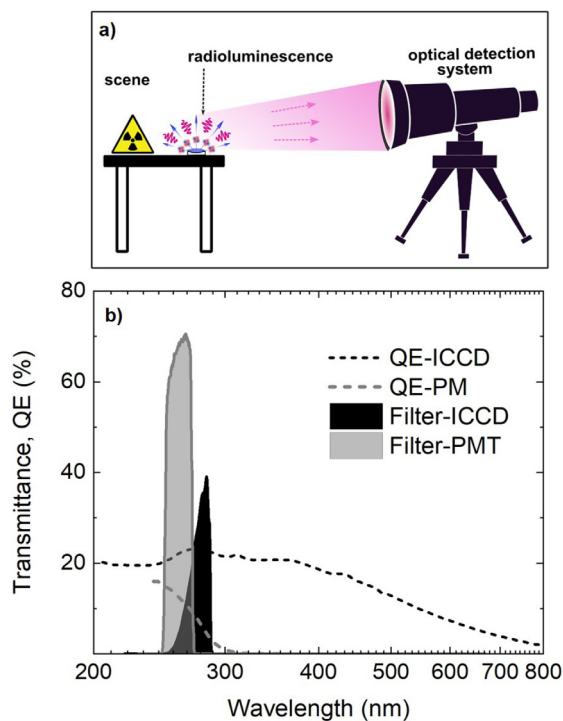

Fig. 1. (color online) (a) Schematic of the UV-C imaging setup. Radioactive material is placed either on the table or inside a steel chamber. The detection system is placed between 0.4 to 0.53 m away from the sample. (b) Quantum efficiency curves of the used detectors (ICCD camera and cesium-telluride photocathode photomultiplier tube) and transmission of the UV-C filters.

intensifier, controlled with the voltage applied to the MCP, has a tuning range between 0 and 4095 (12-bit D/A) with a maximum voltage of 1000 V. Here the gain was set to 3644. This camera also utilizes cooling of the sensor to reduce dark current, however the most significant noise contribution is the thermal emission of electrons from the photocathode and therefore, the best noise reduction would be achieved by cooling the photocathode. During the experiments, no photocathode cooling was applied but the sensor was electrically cooled to −30 °C. The image processing involves (a) subtraction of the no-source (dark level) image from the UV-C image and (b) application of a median filter with a window size of 20 pixels to smooth pixel fluctuation. The last step of the image processing is meant only for displaying the contamination and it is not applied when performing the signal-to-noise ratio (SNR) calculations. SNR was calculated as the quotient of the averaged pixel value in the source region of interest to the background noise level (standard deviation) in a region far from the source [9]. All images were acquired during 2 h integration time (120 exposures, each 60 s long). A 2×2 binning with an equivalent pixel size of 27×27 μm^2 has been proven to provide the best compromise between spatial resolution and signal to noise ratio. The alpha emitting samples imaged using this setup included a 1×5 cm^2 long stripe Am-241 sample with an activity of 32 MBq and, two disk samples with diameter of 1 cm, both Am-241, with activities of 3.7 MBq and 9.9 kBq (a smoke detector ionizer) placed on a chamber with quartz window flushed constantly with a mixture of N$_2$ and NO gases.

2.2. Scanning PMT system

This optical system is based on the Galilean telescope design, with the objective lens having a diameter of 100 mm [7,10]. The telescope is optimized for high light throughput, and to operate with standard 25 mm diameter filter set. The filter set consists of three UV-C filters (FF01-260/16-25, Semrock Inc) with a pass-band close to 260 nm

(see Fig. 1b). The filters are placed between the eyepiece lens and a focusing lens which collects the light onto a cesium-telluride photocathode PMT (H11870-09, Hamamatsu). This photocathode type has a minimal response to wavelengths above 320 nm (1b). The telescope was mounted on a motorized pan–tilt head for scanning the radioluminescence from the sample. The field of view of the scanner allowed to see an area at the imaging plane having diameter of 4 cm. The acquisition time per point was 30 s. The sample imaged with a scanner was a 19.1×11.9 cm^2 wide area reference source composed of natural uranium with a total activity of 330 Bq that yielded to a measured surface emission rate of 150 alphas per second in 2π steradian. The sample was flushed with a N$_2$/NO mixture.

3. Experimental results and discussion

Radioluminsecence imaging is a convenient tool for detecting contaminations with alpha-emitting radionuclides from a distance, without exposing personnel and devices to the radiation itself. In both imaging approaches employed in this study, the UV-C radioluminescence image is superimposed on the conventional image obtained under normal lighting. The conventional image provides coordinates for the contamination and the UV-C image contains quantitative information on the activity of the alpha emitter, since the intensity of radioluminescence is proportional to the total energy loss in air of the alpha particles.

3.1. CCD-based imaging

Fig. 2 shows the radioluminescence image of a 32 MBq, extended Am-241 source obtained in the illuminated lab environment using the CCD-based imaging system. The radioluminescence light emission occurs around the alpha source, in a volume with an extension roughly equal to the alpha particle range measured in air (4.11 cm for americium-241). The UV-C light originates mainly from a very small fraction of N$_2$ radioluminescence which is emitted in the deep UV regime, reaching wavelengths as short as 260 nm. The signal-to-noise ratio of the 32 MBq image is about 3.5. A nearby 3.7 MBq source, on the other hand, was not resolved due to the overwhelming background contribution from the strong source. In general, however, since only trace amounts of the NO molecules in the air and a small portion of the nitrogen emission contribute to signal at wavelengths shorter than 280 nm, the number of radioluminescence photons in the UV-C spectral region is about two order of magnitude lower than that at UV-A and UV-B [7]. This will effectively restrict optical detection of weaker alpha sources.

To enable sensing of radiological threats at a safe distance, appropriate conditions around alpha sources need to be created that favor the production of large amounts of NO radioluminescence. This can be achieved by purging the atmosphere around the alpha emitter with N$_2$ and trace amounts of NO [11,12,14,15]. Nitric oxide (NO) is known to emit light that is almost exclusively located in the UV-C spectral region between 205 and 280 nm. In Fig. 3 we show UV-C radioluminescence imaging of 3.7 MBq source and a photograph of the sample in the experimental chamber. The source was placed on a steel chamber with a quartz window which was flushed with a scientific grade N$_2$ at a rate of 5 L/min (the details of the gas injection system such as mass flow controllers, gas exhaust and mechanical valves can be found on a separate paper by Kerst and Toivonen [14]). The NO volume concentration has been measured to be 50 ppb using a chemiluminescence analyzer, calibrated using a N$_2$ gas sample with a known NO concentration. From the image it is evident that the nitrogen purge with trace amounts of NO enhances substantially the UV-C radioluminescence. The pixel intensity in the image is about hundred times larger relative to the case when the sample is imaged in air. Due to the symmetric geometrical shape of the sample (a disk with 10 mm diameter), the radioluminescence image of the source has the form of a scintillation bubble that can be approximated to a sphere.
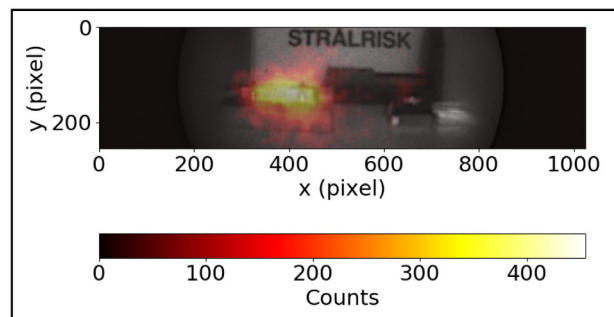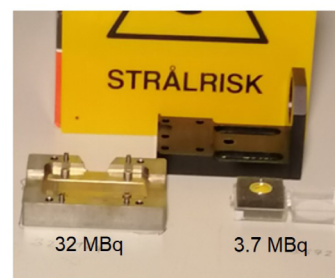

Fig. 2. (color online) UV-C image of a 32 MBq extended alpha source (1×5 cm^2) acquired with ICCD camera (lower panel) and the photograph of the scene (upper part). The UV-C image is superimposed on the CCD image obtained–without filter–under normal lighting. The effective CCD pixel size is 27×27 μm^2.

By adding as little as 3 ppm NO to N$_2$ atmosphere the detection limits can be significantly enhanced. Fig. 4 shows the radioluminescence image of a 9.9 kBq smoke detector ionizer. The sample was flushed with N$_2$ (6.0 purity) at a rate of 5 L/min mixed with trace amounts of NO corresponding to a concentration of 3 ppm.[1] With the setup used in this work we could control the NO level to an accuracy and repeatability of better than 1 ppb. The stability of the signal, however, is merely determined by the detection system itself (thermoionic emission in the photocathode) rather than small fluctuations in the NO concentration. The signal-to-noise ratio (SNR) is about 2 and, as in the previous image, we observe a huge increase of the UV-C signal relative to the air radioluminescence (about 300 fold). The increase of the signal in the NO/N$_2$ mixture is due to excitation transfer from N$_2$ to NO. In this process, molecular nitrogen in the long-lived N$_2$ $A^3\Sigma_u^+$ state excites ground state nitric oxide to NO $A^2\Sigma^+$ state, while the N$_2$ molecule loses its excitation and decays to the ground state [11]. Since the emission efficiency of NO is determined by quenching due to oxygen and water vapor, a nitrogen purge with adequate levels of NO impurities is crucial for the UV-C radioluminescence amplification.

The radioluminescence imaging setup can be further optimized by increasing its geometrical efficiency which is inversely proportional to the square of the detection distance; Fig. 5 shows the simulated radioluminescence signal [8] as a function of source-to-detector distance (d), normalized to the signal measured at 0.5 m with receiving optics diameter of $D_{opt} = 50$ mm, for a scintillation source of 4 cm diameter. The curves have been calculated using the inverse square law with

---

[1] Nitric oxide is highly reactive, oxidizing gas with an irritating odor. Nitric oxide forms acids in the respiratory system which are irritating and cause congestion in the lungs. Concentrations of 60–150 ppm cause immediate irritation of the nose and throat while concentrations of 200–700 ppm may be fatal after very short exposure [23]. In the European Union the occupational exposure limits over an 8-hour time weighted average (TWA) is 2 ppm [24]. TWA can be used when both the chemical concentration and time for exposure varies and it indicates the average exposure to a contaminant to which workers may be exposed without adverse effect over a period such as in an 8-hour day. In the US, the recommended exposure limit over an 8-hour workday is set to 25 ppm [25].
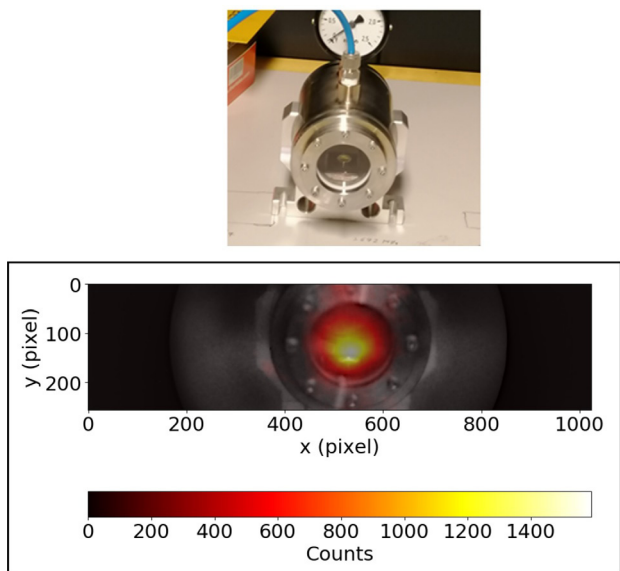
Fig. 3. (color online) UV-C radioluminescence imaging of 3.7 MBq source (lower panel) and a photograph of the sample in the experimental chamber (upper part). The alpha source was placed on a steel chamber with a quartz window, flushed with N_2 (6.0 purity) at a rate of 5 L/min. The NO concentration was 50 ppb.
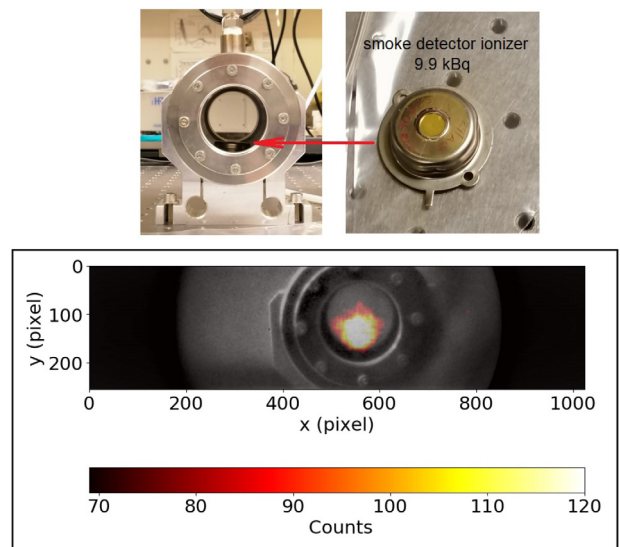

Fig. 4. (color online) UV-C radioluminescence image of a 9.9 kBq smoke detector ionizer. The concentration of NO at the N_2 atmosphere was about 3 ppm.

the solid angle for a disk source parallel to a detector with a circular aperture [26]. Signal losses due to the increase of the detection distance can be compensated by using large receiving optics. For example, the signal measured at 0.5 m with D_{opt} = 50 mm optics could be measured at 2 m when using a 200 mm diameter optics. Alternatively, with 200 mm receiving optics placed 0.5 m from the source we can image a source with an activity as low as 700 Bq. The practical limit for compensating an increase in detection distance by a larger collection optics depends on the weight and the size of the optical detection system, and the platform such system is integrated. For example, optical detection systems based on aluminum paraboloid-reflectors are light weight and, therefore, even reflectors with diameters as large as 500 mm can be easily accommodated into a robotic vehicle, drones or tripod systems. Optical detection systems composed of fused silica lenses, on the other hand, are heavier, but even in this case lenses with diameter as large
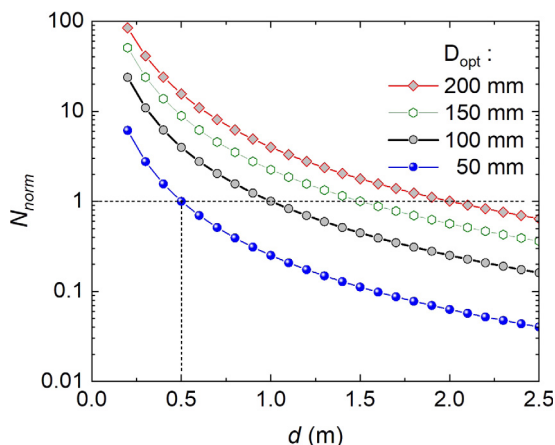

Fig. 5. (color online) In optical alpha particle detection, the radioluminescence signal decreases with the well-known geometric scaling where the signal level is inversely proportional to the square of the detection distance (d). Signal losses due to the increase of the detection distance can be compensated by using receiving optics with larger diameter (D_{opt}).
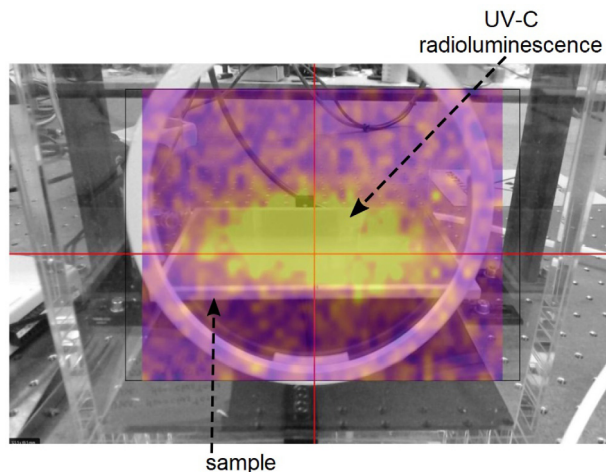

Fig. 6. (color online) Image of a wide area reference alpha-emitting source composed of the uranium isotopes U-234, U-235 and U-238, with a total activity of 330 Bq over an active area of 19.1 × 11.9 cm². The concentration of NO at the N_2 atmosphere was about 3 ppm. The scene was scanned using scanning PMT system at about 0.4 m distance with a resolution of 1 deg and 30 s integration per point.

as 240 mm are available, and the whole optical system can be easily accommodated in different motorized platforms. The field of view of the detection system should not be an issue of concern since the grid of overlapping scan points can always be interpolated to create a continuous contamination map.

3.2. Scanner-based imaging

The scanning PMT system has been designed with a ray tracing software and optimized for high light throughput. Having a 100 mm receiving optics, its geometrical efficiency is a factor of four larger than that of the CCD-based imaging system, and thus capable of imaging contaminations with activities below 1 kBq. Fig. 6 shows the radioluminescence imaging of a 330 Bq wide area reference source with a specific activity of about 1.5 Bq/cm². The sample is placed into a gas tight chamber which has a UV fused silica window. The sample was flushed with N_2 (5.0 purity) at a rate of 5 L/min with 3 ppm trace amount of NO. From the figure it is evident that, even at such a low specific activity, the radioluminescence was still visible, with

an average signal level of about 75 cps and a noise level of about 31 cps. To the best of our knowledge, this is the lowest activity imaged using UV-C radioluminescence to date. The present results indicate that optimizing such imaging techniques can push the detection limit even further down and such techniques might also be used for determination of legal limits in the future.

4. Conclusion

Our measurements show that by using adequate levels of nitric oxide impurities in the N_2 gas atmosphere surrounding the alpha source, low activity samples, such as those used in smoke detector ionizers and surface contaminations of an activity as low as about 330 Bq can be imaged in the UV-C spectral region. Adding as low as 3 ppm NO in a N_2 gas, the signal enhancement can be more than three orders of magnitude relative to the atmospheric radioluminescence. These results demonstrate that both camera- and scanner-based detection technologies in conjunction with a proper N_2/NO atmosphere have the potential to evolve into a standard procedure in the nuclear industry sector. This is especially important as it shows promise for the detection under normal illumination. This includes nuclear facilities, where isotopes are produced, handled, used and stored. It seems feasible, for example, to flood GLOVE-boxes with a proper N_2/NO mixture and map constantly whereabouts of all alpha sources by imaging the emanating UV-C light, or to flood a contaminated area in a nuclear facility and quickly localize the sources of alpha radiation while keeping personnel at a safe distance. Similarly, this method can be also applied for inspecting installations during decommissioning of old nuclear facilities. It should however be emphasized that radioluminescence in air (or gases) is not useful for the detection of gamma emitters because the intensity of air radioluminescence is inversely proportional to the third power of the mean free path of the ionizing radiation particle, and therefore, the brightness of radioluminescence induced by gamma rays is low [6]. For high-energy beta emitters, such as Sr-90, the situation resembles that of gamma rays. However, with low-energy beta particles, Ni-63 in particular, the alpha imaging techniques may have some power — but at the moment no scientific evidence exists. By using large collection optics we can compensate signal losses due to geometrical scaling and thus increase the detection distance. Moreover, both security officials and regulatory authorities need such detection tools for crime scene investigation (including illicit trafficking of alpha emitting radioactive material) and possible large scale radiological emergencies. In the case of large scale radiological emergencies involving accidental or deliberate dispersion of alpha emitting radionuclides into the environment , depending on their distribution pattern and meteorological conditions such as wind and precipitation, large areas could be contaminated. By combining optical detection with the wireless data collection and transmission technology, one overcomes all drawbacks of the conventional detection techniques such as (i) keeping both the operator and the equipment out of the danger zone, (ii) providing real-time information on the source location and morphology, and (iii) assist on the on-site incident management, evacuation plans as well as in developing strategies for protecting public from harm [27]. Radioluminescence detection systems can be installed into a multi-rotary-wing unmanned airborne vehicles. These vehicles can be chosen with sufficient payload and flying range according to the weight of the optical detection system and, can be optimized to carry properly the detector and hover with good stability. Depending on the activities of the contaminating radionuclides and the size of the collection optics, one may flood of the contaminated area with gases such as N_2–NO mixture to enhance the detection limit.

CRediT authorship contribution statement

Faton S. Krasniqi: Designed and performed the experiments, Wrote the manuscript, Discussed the results, Contributed to the final manuscript. **Thomas Kerst:** Designed and performed the experiments, Discussed the results, Contributed to the final manuscript. **Martti Leino:** Designed and performed the experiments, Discussed the results, Contributed to the final manuscript. **Jens-Tarek Eisheh:** Designed and performed the experiments, Discussed the results, Contributed to the final manuscript. **Harri Toivonen:** Designed and performed the experiments, Discussed the results, Contributed to the final manuscript. **Annette Röttger:** Aided in interpreting the results, Discussed the results, Contributed to the final manuscript. **Juha Toivonen:** Designed and performed the experiments, Wrote the manuscript, Discussed the results, Contributed to the final manuscript.

Declaration of competing interest

The authors declare that they have no known competing financial interests or personal relationships that could have appeared to influence the work reported in this paper.

Acknowledgments

References

[1] J. Shapiro, Radiation Protection—A Guide for Scientists, Regulators and Physicians, fourth ed., Harvard University Press, 2002.

[2] D.I. Chanin, W.B. Murfin, Site restoration: Estimation of attributable costs from plutonium-dispersal accidents, SAND–96-0957, United States, 1996.

[3] L.A. Burchfield, Radiation Safety: Protection and Management for Homeland Security and Emergency Response, Wiley, 2009.

[4] E.B. Podgorsak, Radiation Physics for Medical Physicists, Springer, 2010.

[5] J.M. Thompson, Tracking down alpha-particles: The design, characterisation and testing of a shallow-angled apha-particle irradiator, Radiat. Prot. Dosim. (2019).

[6] S.M. Baschenko, Remote optical detection of alpha particle sources, J. Radiol. Prot. 24 (2004) 75.

[7] J. Sand, Alpha Radiation Detection Via Radioluminescence of Air, Vol. 1449 (Ph.D. thesis), Tampere University of Technology, Tampere, Finland, 2016.

[8] J. Sand, S. Ihantola, K. Peräjärvi, H. Toivonen, J. Toivonen, Radioluminescence yield of alpha particles in air, New J. Phys. 16 (2014) 053022.

[9] J. Sand, Ihantola S., A. Nicholl, K. Peräjärvi, H. Toivonen, J. Toivonen, Imaging of alpha emitters in a field environment, Nucl. Instrum. Methods Phys. Res. A 782 (2015) 13.

[10] J. Sand, A. Nicholl, E. Hrnecek, H. Toivonen, J. Toivonen, Peräjärvi, Stand-off radioluminescence mapping of alpha emitters under bright lighting, IEEE Trans. Nucl. Sci. 63 (2016) 1777.

[11] T. Kerst, J. Toivonen, Intense radioluminescence of NO/N_2-mixture in solar blind spectral region, Opt. Express 26 (2018) 33764.

[12] T. Kerst, Optical Stand-Off Detection of Alpha Radiation in Nuclear Facilities (Ph.D. thesis), Tampere University, Tampere, Finland, 2019, Tampere University Dissertations 129.

[13] A.J. Crompton, K.A.A. Gamage, A. Jenkins, C.J. Taylor, Alpha particle detection using alpha-induced air radioluminescence: A review and future prospects for preliminary radiological characterisation for nuclear facilities decommissioning, Sensors 18 (2018) 15.

[14] T. Kerst, J. Toivonen, Dynamic enhancement of nitric oxide radioluminescence with nitrogen purge, Sci. Rep. 9 (2019) 13884.

[15] T. Kerst, J. Sand, S. Ihantola, K. Peräjärvi, A. Nicholl, E. Hrnecek, H. Toivonen, J. Toivonen, Standoff alpha radiation detection for hot cell imaging and crime scene investigation, Opt. Rev. 25 (2018) 429.

[16] J. Yao, J. Brenizer, R. Hui, S. Yin, Standoff alpha radiation detection via excited state absorption of air, Appl. Phys. Lett. 102 (2013) 254101.

[17] D. Kim, D. Yu, A. Sawant, M.S. Choe, I. Lee, S.G. Kim, E.M. Choi, Remote detection of radioactive material using high-power pulsed electromagnetic radiation, Nature Commun. 8 (2017) 15394.

[18] P. Sprangle, B. Hafizi, H. Milchberg, G. Nusinovich, A. Zigler, Active remote detection of radioactivity based on electromagnetic signatures, Phys. Plasmas 21 (2014) 013103.

[19] K. Konthasinghe, K. Fitzmorris, M. Peiris, A.J. Hopkins, B. Petrak, D.K. Killinger, A. Muller, Laser-induced fluorescence from N_2^+ ions generated by a corona discharge in ambient air, Appl. Spectrosc. 69 (2015) 1042.

[20] F. Lamadie, F. Delmas, C. Mahe, P. Gironès, C. Le Goaller, J.R. Costes, Laser-induced fluorescence from N_2^+ ions generated by a corona discharge in ambient air, IEEE Trans. Nucl. Sci. 52 (2005) 3035.

[21] O.P. Ivanov, V.E. Stepanov, S.V. Smirnov, Volkovich A. G., Development of method for detection of alpha contamination with using UV-camera "DayCor" by OFIL, in: Nuclear Science Symposium and Medical Imaging Conference, NSS/MIC, IEEE, Valencia, 2011, pp. 2192–2194.

[22] T. Kerst, R. Malmbeck, N. Banik, J. Toivonen, Alpha radiation-induced luminescence by Am-241 in aqueous nitric acid solution, Sensors 19 (2019) 1602.

[23] NIH, US national institute of health, PubChem: Nitric oxide, 2020, https://pubchem.ncbi.nlm.nih.gov/compound/Nitric-oxide.

[24] E.C. SCOEL, European commission SCOEL/SUM/89 June 2014, recommendation from the scientific committee on occupational exposure limits for nitrogen monoxide, 2014.

[25] NIOSH, The national institute for occupational safety and health: Nitric oxide, 2020, https://www.cdc.gov/niosh/npg/npgd0448.html.

[26] G.F. Knoll, Radiation Detection and Measurment, fourth ed., Wiley, 2017.

[27] RemoteALPHA, Remote and real-time optical detection of alpha-emitting radionuclides in the environment, 2020, https://www.euramet.org/research-innovation/search-research-projects/details/project/remote-and-real-time-optical-detection-of-alpha-emitting-radionuclides-in-the-environment/.